

EXPERIMENTAL STUDY ON STRUCTURAL PERFORMANCE AND DAMAGE MITIGATION OF RC COLUMNS USING HYBRID FIBER REINFORCED CEMENT-BASED COMPOSITES

Joji SAKUTA¹, Yusuke TANABE², Masaki MAEDA³, and Hirozo MIHASHI⁴

¹ Research Associate, Dept. of Architecture and Building Science, Tohoku University, Sendai, Japan

² Takenaka Corporation, Osaka, Japan

³ Associate Professor, Dept. of Architecture and Building Science, Tohoku University, Sendai, Japan

⁴ Professor, Dept. of Architecture and Building Science, Tohoku University, Sendai, Japan

Email: sakuta@archi.tohoku.ac.jp

ABSTRACT :

As a kind of Ductile Fiber Reinforced Cementitious Composites (DFRCC), Hybrid Fiber Reinforced Cement-based Composites (HFRCC) have been developed. HFRCC includes two kinds of fibers, which are short and thin synthetic fibers such as Polyethylene or Polyvinyl Alcohol fibers and long fibers such as steel cords. Short fiber reinforces micro cracks while long does mezzo cracks, so that cracks disperse and each fiber works in different strain level. By applying HFRCC instead of Concrete to structural members, not only improvement of structural performance but also mitigation of damage under seismic loads would be expected.

In this paper, static cyclic tests of columns are carried out to investigate seismic capacity and effect of damage control of HFRCC. Variables of test specimens are materials, the quantity of lateral reinforcement, and axial load condition. Usage of HFRCC are concluded as improvement of structural performance such as ductility, shear resistance, axial load carrying capacity, mode of failure, and damage level due to multiple cracks, pseudo strain hardening, and ductile tensile behavior by experimental study. Furthermore, it is shown that shear resistance and load carrying capacity can be evaluated by adding the effect of tensile strength of HFRCC to lateral reinforcement strength of conventional design formula.

KEYWORDS: HFRCC, Damage Mitigation, Multiple Cracks, DFRCC, RC Column, Ultimate Shear Strength

1. INTRODUCTION

Hybrid Fiber Reinforced Cement-based Composites (HFRCC) includes two kinds of fibers, which are short thin fibers and long fibers. Bending characteristics of HFRCC materials shown in Figure 1 have proved that two fibers contribute to improve tensile behavior of mortar without brittle fractures. Even after the initial crack occurs, flexural moment increases until the multiple cracks localize. Recently, many types of DFRCC were introduced in JCI (2002) and also the effect of damage mitigation was shown in FUKUYAMA (2006). To control the crack width narrow in structural members, it is also important for HFRCC to control the strain before cracks localize.

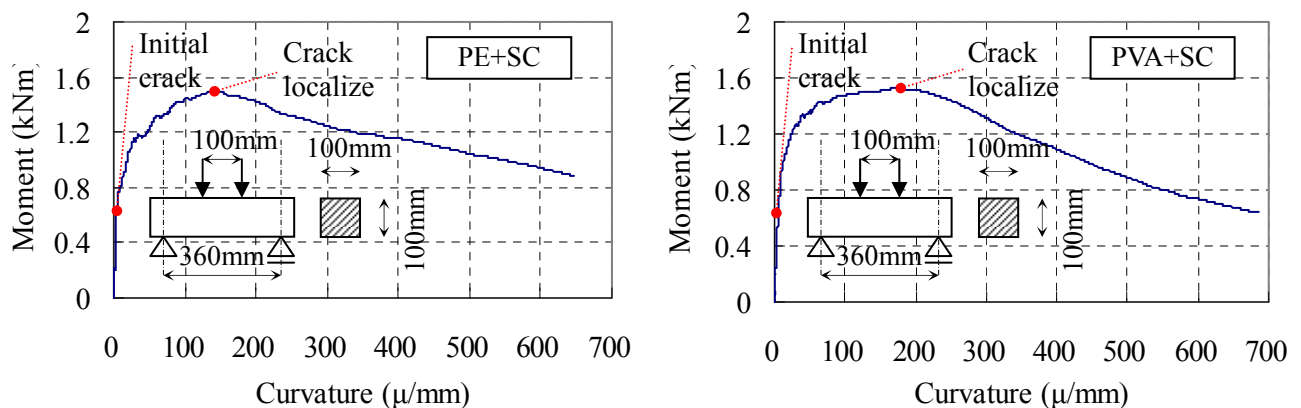


Figure 1 Moment-Curvature relationship of HFRCC

Static cyclic tests of columns were conducted to investigate effect of HFRCC on seismic capacity and damage control. While five columns were tested under constant axial load, two columns were tested under varying high axial compression and tension acting simultaneously with shear and flexure, assuming the column in the soft first story of a building, in which generally the most severe load condition to columns is expected.

In this paper, the experimental study comparing RC to HFRCC columns are reported.

2. COLUMNS UNDER CONSTANT AXIAL LOAD

Cyclic loading tests of five columns are conducted under constant axial load to compare shear failure behavior of RC to HFRCC columns. In this chapter, by showing shear versus drift angle relationship and damage level in each drift angle using crack widths research, improvements of structural performance such as ductile deformation capacity and change of failure mode from shear to flexure are proved. Furthermore, the mitigation of damage is observed in HFRCC against RC columns.

2.1. Test Specimens

The dimensions and the reinforcing arrangements of test specimens are shown in Table 2.1 and Figure 2.1. Variables in this test are types of cementitious material and quantities of lateral ties.

The three types of cement materials are used, which is normal concrete, mortar with PE+SC, and mortar with PVA+SC. PE, PVA, and SC represent Polyethylene, Polyvinyl Alcohol, and Steel Cord, respectively. The mortar of HFRCC has a water-cement ratio of 45% and a sand-cement ratio of 45%. The volume ratio of 0.75% polyethylene fibers and 0.75% steel cords are mixed for HF-PE series while 0.75% polyvinyl alcohol fibers are used instead of PE for HF-PVA. Also, three different quantities of lateral ties are placed such as none of ties, D6 deformed rebar (6mm diameter) used in 160 mm spacing, and D6 used in 80 mm spacing. p_w (%) shown in Table 2.1 is calculated from the area of lateral ties divided by the spacing and width of columns.

Test specimens are named from the kinds of cementitious material and lateral ties ratio (p_w). Longitudinal reinforcements are the same in all test specimens, and then the calculated bending capacity is equal in every specimen under the same constant axial load.

Table 2.1 Test specimens

Name of specimen	Cementitious material	Fiber	Cross section	Clear span	Main bar (p_g %)	Hoop	
						#-Size@space	p_w (%)
N-02	Concrete	None	200 x 400 (mm)	800 (mm)	4-D16 (1.00%)	2-D6@160	0.20
N-04						2-D6@80	0.40
HF-PE-00	HFRCC	PE+SC	200 x 400 (mm)	800 (mm)	4-D16 (1.00%)	None	0.00
HF-PE-02		PVA+SC				2-D6@160	0.20
HF-PVA-02						2-D6@160	0.20

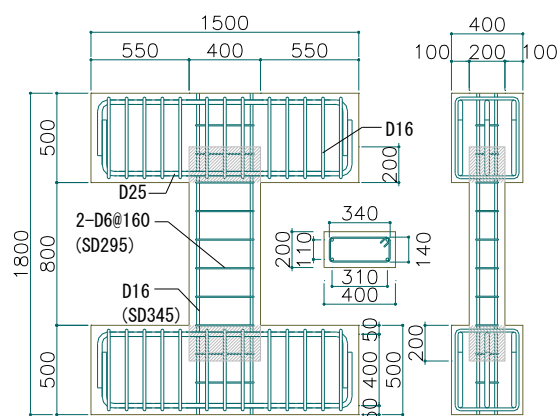


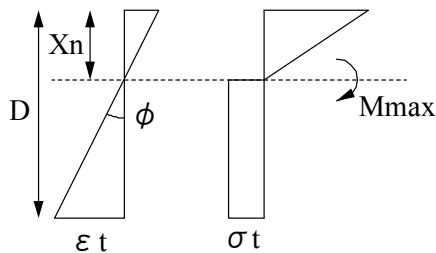
Figure 2.1 Test specimens with Hoop $p_w = 0.2$ % series

The material properties are shown in Table 2.2. Compressive strength was obtained from the compression test results of cylinder pieces of 100mm diameters x 200mm heights. Tensile strength of concrete was obtained from the same cylinder specimens using the method of splitting tensile test, but that of HFRCC was given from the bending test results shown in Figure 1 using JCI method JCI-S-003-2005 (Test method for bending moment-curvature curve of fiber reinforced cementitious composites). Figure 2.2 shows the assumption of stress distribution in cross section applied to calculation of ultimate flexural moment from which tensile strain and tensile strength were evaluated from bending test by Eqn. 2.1.

Table 2.2 Material properties

Cementitious material					Steel bar			
Type	Fiber	Compressive strength (N/mm ²)	Young's modulus (×10 ⁴ N/mm ²)	Tensile strength (N/mm ²)	Size	Yield stress (N/mm ²)	Yield strain (μ)	Tensile strength (N/mm ²)
Concrete	None	52.8	2.36	3.83	D16	371	2132	537
HFRCC	*PE+SC	55.3	1.85	3.40	D6	284	1988	455
	*PVA+SC	56.8	2.05	3.41				

*PE: Polyethylene fibers 0.75 vol. %, *PVA: Polyvinyl alcohol fibers 0.75 vol. %, *SC: Steel cords 0.75 vol. %



$$\begin{aligned} \varepsilon_t &= \phi D(1 - x_{n1}) \\ \sigma_t &= \frac{E\phi D X_{n1}^2}{2(1 - X_{n1})} \\ X_{n1} &= \frac{X_n}{D} \\ E &: \text{Young's modulus} \end{aligned} \quad (2.1)$$

Figure 2.2 Stress distribution of HFRCC

2.2. Test Methods

The loading set up at experimental laboratory of Tohoku University is shown in Figure 2.3. Two vertical hydraulic jacks with 1000kN capacity applied total constant axial load of 450kN (axial stress is 10% of concrete compressive strength σ_B), and one horizontal jack with 1000kN capacity applied cyclic lateral load to the steel frame for loading at the mid-height of column specimens under displacement control condition shown in Figure 2.4.

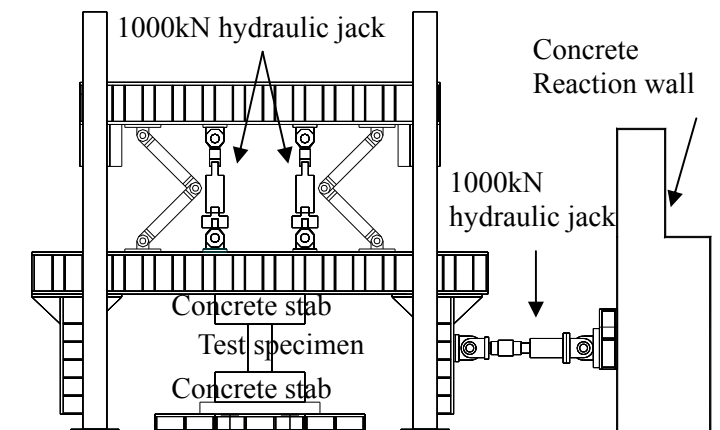


Figure 2.3 Loading set up

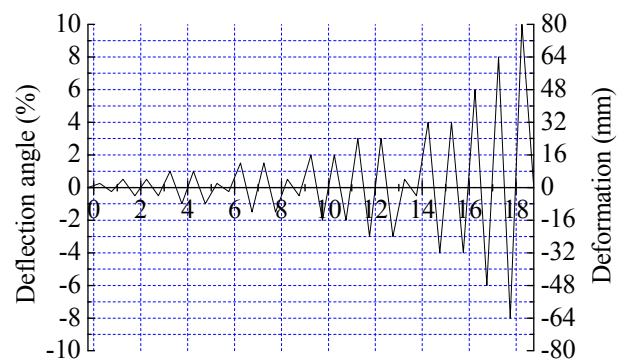


Figure 2.4 Loading hysteresis

2.3. Test Results

Shear versus drift angle relationship with calculated shear and bending capacity, the state of final failure, maximum shear crack width in each drift angle, and strain in lateral ties are shown in this section.

2.3.1 Shear versus drift angle

Figure 2.5 shows the relationship between shear force and drift angle, and the state of ultimate failure of each test specimen. N-02 and N-04 showed a decrease in strength due to shear failure at relatively small drift angle while all the HFRCC columns showed a good ductility without decrease in shear force until a drift angle of 1/10rad. sustaining constant axial forces. Shear failure in N-02 occurred at the first cycle of drift angle of 1/200rad. and in N-04 occurred at the first cycle of drift angle of 1/67rad. It was impossible for both N-02 and N-04 test specimens to support axial load at the time of shear failure, so the loading finished at that cycle. On the other hand, even under the maximum axial force of 2000kN of maximum loading capacity of vertical jacks after drift angle of 1/10rad., HFRCC test specimens stayed at the elastic range in the vertical direction and supported the axial load safely.

The calculated bending capacity and shear capacity taking tensile strength of HFRCC into calculation was also shown in Figure 2.5. The calculation of ultimate shear strength is given by Eqn. 2.2 referring to AIJ (1990) and NAGAI et al. (2004). By comparing calculation to the test results, it can be concluded that tensile stress in HFRCC contributed to improvement of shear capacity as lateral reinforcement does. Then, mode of failure changes and structural performance is improved.

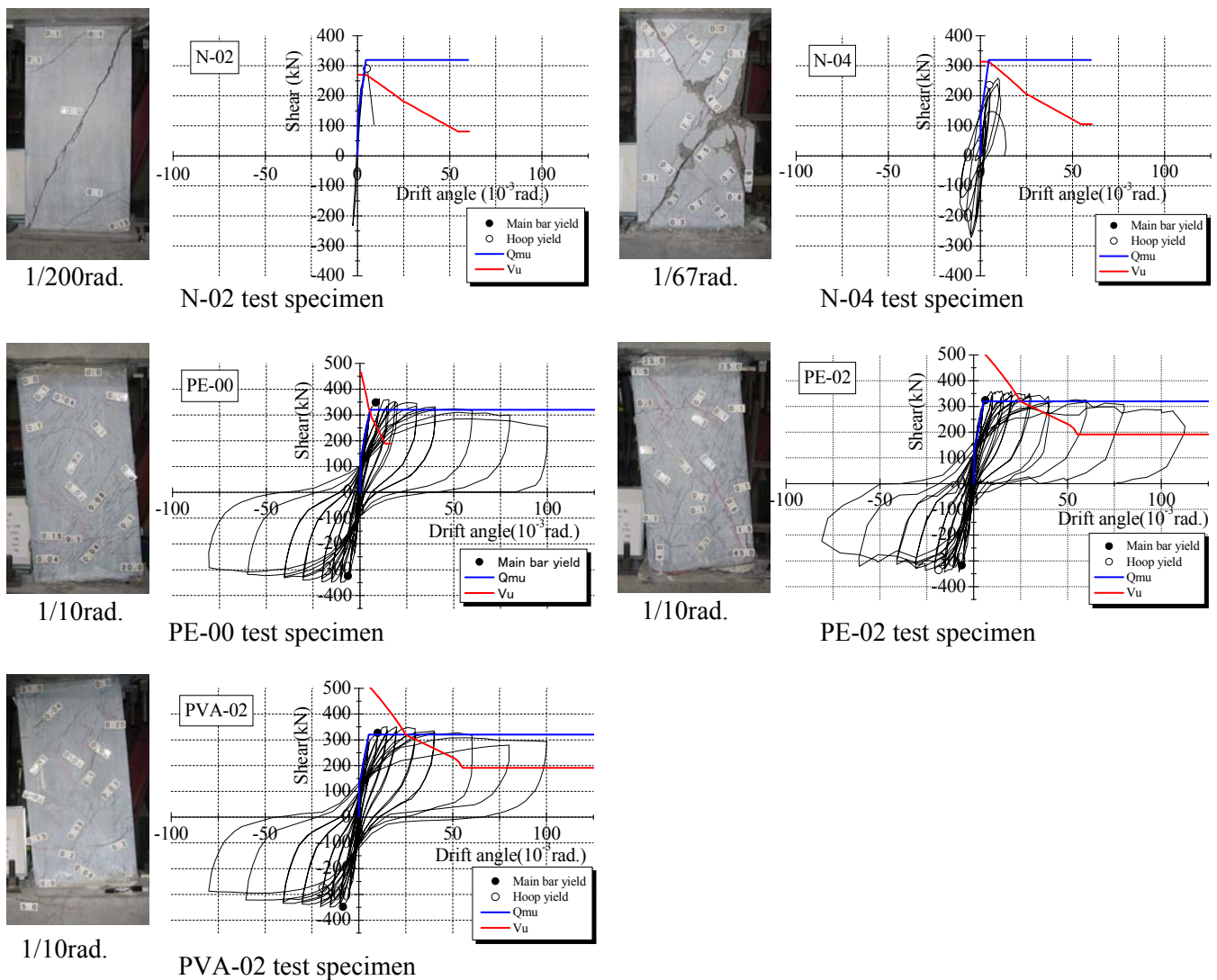


Figure 2.5 Shear and drift angle relationship

$$V_{su} = b j_t (p_w \sigma_{wy} + \sigma_t) \cot \phi + \tan \theta (1 - \beta) b D v \sigma_B / 2 \quad (2.2)$$

$$\tan \theta = \sqrt{(L/D)^2 + 1} - L/D$$

$$\beta = \{(1 + \cot^2 \phi)(p_w \sigma_{wy} + \sigma_t)\} / (v \sigma_B)$$

p_w : Lateral ties ratio

σ_{wy} : Yield strength of lateral ties

$$v = (1.0 - 15R_p)v_0 \quad 0 < R_p < 0.05$$

$$v = 0.25v_0 \quad 0.05 < R_p$$

$$v_0 = 1.7\sigma_B^{1/3}$$

σ_t : Tensile Strength of HFRCC

b, D, L : width, Depth, and Length of column

$$\cot \phi = \min(\cot \phi_1, \cot \phi_2, \cot \phi_3)$$

$$\cot \phi_1 = 2 - 50R_p \quad 0 < R_p < 0.02$$

$$\cot \phi_1 = 1 \quad 0.02 < R_p$$

$$\cot \phi_2 = j_t / (D \tan \theta)$$

$$\cot \phi_3 = \sqrt{v \sigma_B / (p_w \sigma_{wy} + \sigma_t)} - 1.0$$

2.3.2 Damage behavior

Figure 2.6 shows the relationships between maximum residual shear crack width and drift angle. Although crack width suddenly propagates wider after shear failure in reinforced concrete columns, crack width kept less than 0.3 mm in HFRCC columns due to multiple shear cracks. It proves the damage mitigation that HFRCC remarkably reduces the damage of columns. Figure 2.7 shows the relationship between peak bending cracks and drift angle. Flexural crack width in HFRCC test specimens tends to exceed those in RC after 1/100rad. or more because flexural deformation of HFRCC column concentrate to rotation at critical section after localization of flexural cracks.

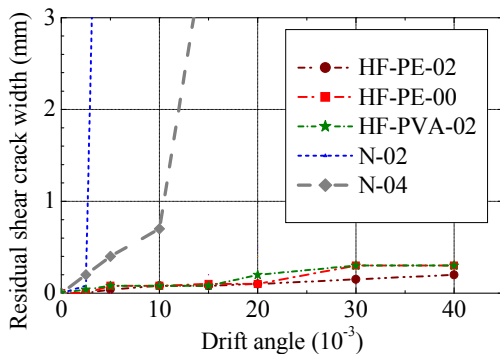


Figure 2.6 Maximum residual shear crack width

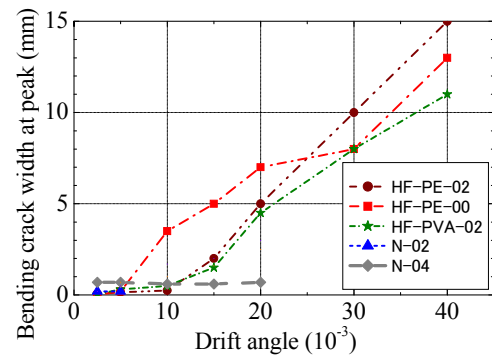


Figure 2.7 Maximum peak bending crack width

2.3.3 Strain at lateral ties

In order to compare strain at lateral ties, three columns with same spacing of lateral ties are chosen and strain distributions are shown in Figure 2.8. The strain of 2000 μm shown in the Figure corresponds to the yield strain of the lateral ties. The lateral ties in reinforced concrete column (N-02) yield at drift angle of 1/200rad., but those in HFRCC columns yield at approx. drift angle of 1/25rad. uniformly from the top through the bottom which shows the effects of tensile strength ductility of HFRCC. Since localization of the shear strain is not observed, concentration of the shear cracks neither occurs.

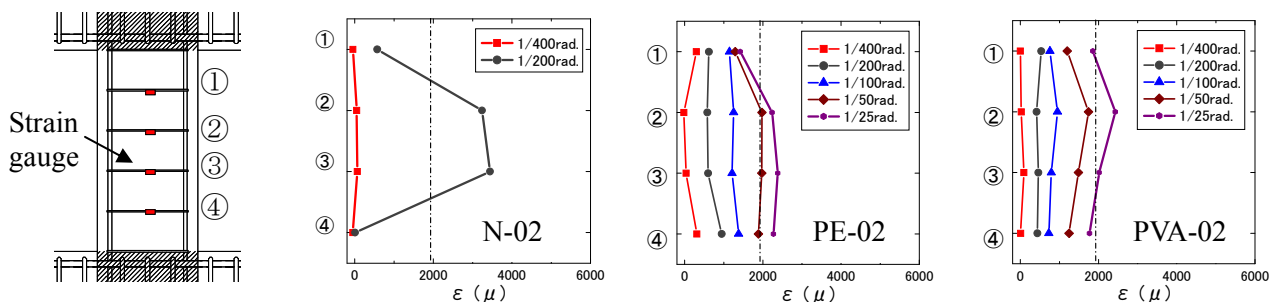


Figure 2.8 Strain of lateral ties

3. COLUMNS UNDER VARYING AXIAL LOAD

Columns in a soft first story are required to perform as ductile members until large deformation because of necessity of energy dissipation at single story instead of dissipation at several stories for building forming the whole yielding mechanism. Cyclic loading tests of two columns are conducted under varying axial load. In this chapter, seismic performance and damages of two columns using the different material RC and HFRCC under varying high axial load with lateral deformations are compared.

3.1. Test Specimens

Cross section of two column specimens and outline of test specimen are shown in Table 3.1. Variables in this test are also types of cementitious material and quantities of lateral ties. The cement materials are concrete and PE+SC. The different quantities of lateral ties are provided such as four D6 deformed rebars spaced at 40 mm spacing, and two D4 deformed rebars spaced at 40 mm spacing. When compared with p_w (%) shown in Table 3.1, lateral ties in reinforced concrete column is provided with five times ties as much as p_w is provided in HFRCC. Test specimens are named from the kinds of cement material. Longitudinal reinforcements are the same in two test specimens, and then the calculated bending capacity is equal in both specimens.

The material properties are shown in Table 3.2. Both compressive strengths and tensile strength of concrete and HFRCC were derived from the same way as shown in Chapter 2.1.

Table 3.1 Test specimens

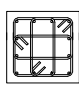
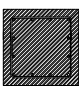
Name of specimen	Section	Cementitious material	Fiber	Cross section (b x D)	Clear span	Main bar (p_g %)	Hoop	
							#-Size@space	p_w (%)
V-N		Concrete	None	250× 250 (mm)	800 (mm)	12-D10 (1.36%)	4-D6@40	1.28
V-HF		HFRCC	PE+SC				2-D4@40	0.25

Table 3.2 Material properties

Cementitious material					Steel bar			
Type	Fiber	Compressive strength (N/mm ²)	Young's modulus ($\times 10^4$ N/mm ²)	Tensile strength (N/mm ²)	Size	Yield stress (N/mm ²)	Yield strain (μ)	Tensile strength (N/mm ²)
Concrete	None	52.6	2.62	2.65	D10	436	4163	655
HFRCC	*PE+SC	51.2	1.81	2.94	D6	337	3710	486
					D4	349	3811	522

*PE : Polyethylene fibers 0.75 vol. %, *SC : Steel cords 0.75 vol. %

3.2. Test Methods

The loading set up is the same as shown in chapter 2, but the axial load is varying as shown in Figure 3.1. Calculation of objective building showed a varying zone of axial load in column as very small deflection range, but it is difficult to control as calculated, so axial load varied in proportion to drift angle within 1/400rad. shown in Figure 3.1. Shear force was applied at the mid-height of columns as shown in chapter 2.

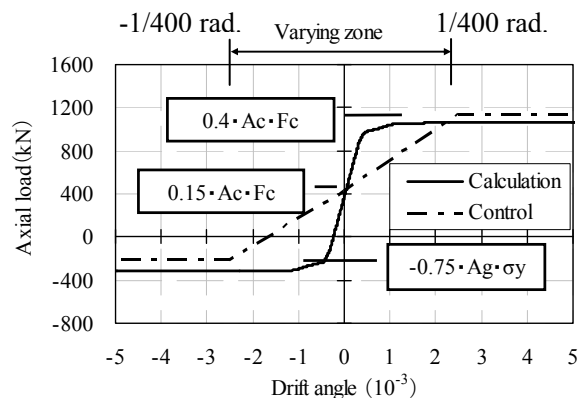


Figure 3.1 Varying axial loads and drift angle relationship

3.3. Test Results

Shear versus drift angle relationship with evaluation of shear and bending capacity and the state of damage are shown in this section.

3.3.1 Shear versus drift angle

Figures 3.2 and 3.3 show the relationships between shear force and drift angle, and the pictures of damage at drift angle of 1/67 and 1/25 rad. I, II, III, IV, and V indicate the damage class based on JBDPA (2001). Damage class I and V correspond to slight damage and collapse, respectively as shown in Figure 3.4. The calculated bending and shear capacity considering tensile strength of HFRCC is also shown together with the test results. The calculation is given by Eqn. 2.1. By comparing calculation to the test results, it can be also concluded that tensile stress in HFRCC contributed to improvement of shear capacity as the lateral reinforcement does even under the condition of varying high axial load.

Although stiffness and maximum shear of V-HF are slightly lower than those of V-N test specimen, V-HF demonstrated ductile deformation capacity up to 1/25rad. in spite of less lateral reinforcement than V-N..

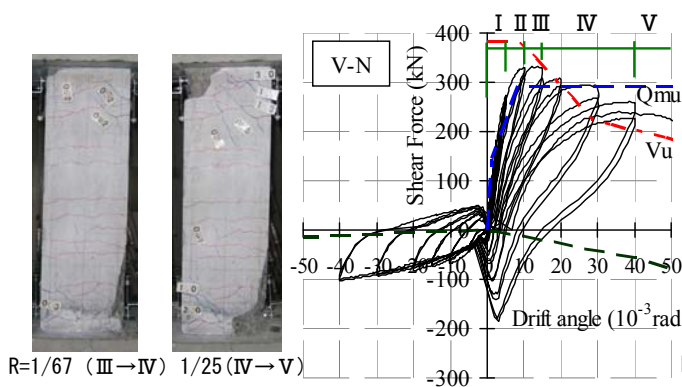


Figure 3.2 Shear-drift angle relationship (V-N)

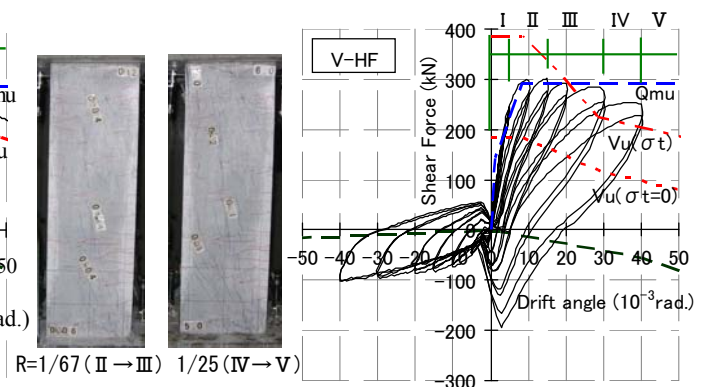


Figure 3.3 Shear-drift angle relationship (V-HF)

3.3.2 Damage behaviors

Figure 3.4 shows general concept of damage level classification employed in JBDPA (2001) and AIJ (2004). Differences in process of damage behavior of both specimens are discussed herein by comparing damage class of V-N and V-HF.

The initial crack occurred at drift angle of 1/800rad. in V-N test specimen of reinforced concrete column (damage level I). At drift angle of 1/200rad., the residual bending crack width was about 0.3mm and shear crack became visible at the peak (damage level I to II). Main bar yielded and some cover concrete spalled at drift angle of 1/100rad. (damage level II to III). Maximum shear force appeared at drift angle of 1/67rad. and the residual bending crack width of 0.8mm and the residual shear crack width of 0.1mm occurred (damage level III to IV). Shear resistance gradually decreased at the cycle of drift angle of 1/50rad. due to spall of the cover concrete, and bending crack width reached 2mm at peak shear and residual crack width was 1.2mm (damage level IV). At the cycle of drift angle of 1/33rad., the residual cracks propagate more and shear forces decreased to 80% of maximum shear mostly due to P-delta effect (still damage level IV). Lateral ties and main bar were exposed at drift angle of 1/25rad., and the shear force did not reach 80% of max. shear force (damage level V).

In V-HF shown in Figure 3.3, the initial crack also occurred at drift angle of 1/800rad. (damage level I). At drift angle of 1/200rad., the residual bending crack width remained about 0.04mm (still damage level I). At the cycle of drift angle of 1/100rad., all the residual shear cracks when unloading closed, but residual bending crack width was 1mm and longitudinal crack width at the compression zone was 0.3mm since the bending cracks concentrated at one critical section (damage level I to II). Shear force reached to the maximum at the peak of first cycle of drift angle of 1/67rad. and the residual concentrated bending crack width of 3mm, but the other crack width remained less than 0.4mm (damage level II to III). Shear capacity slightly decreased at drift angle of 1/50rad. mostly due to P-delta effect and no spall of the cover concrete occurred, but only one concentrated bending crack extended (damage level III). At drift angle of 1/33rad., the residual longitudinal crack width at compression zone was 3mm, and fibers exposed. The one part of residual bending crack width was 7mm, but the other bending crack width was less than 0.5mm (damage level III to IV). The concentrated residual bending

crack extended to 9.5mm and shear force decreased at 80% of the maximum shear force (damage level IV to V). Comparing to the V-N specimen of RC column, the damage of HFRCC was remarkably few during drift angles from 1/200rad. to 1/50rad. because of ductile tension resistance of HFRCC. Spall and crush of cover concrete which is trigger of decrease in bending moment occurred in V-N while neither spall nor crush was observed in V-HF. Though bending cracks finally localized at the critical section and propagated in HFRCC column, other cracks remained very narrow. Shear crack was few in both RC and HFRCC columns since both failed in flexure.

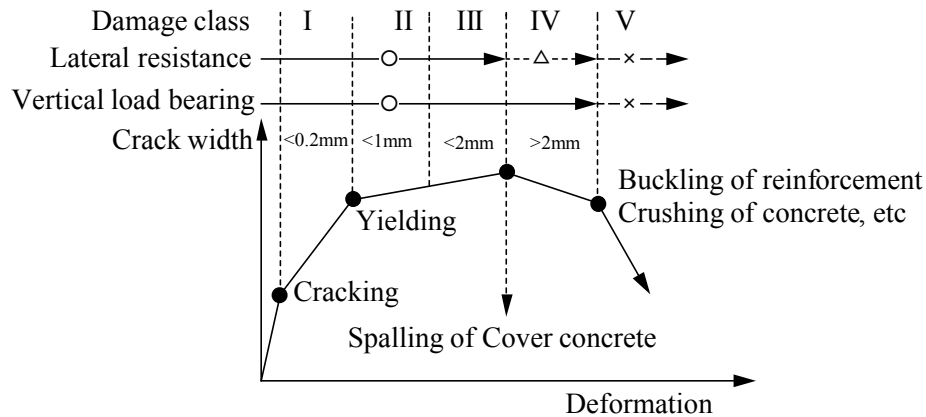


Figure 3.4 Damage level of ductile member

4. CONCLUSIONS

Cyclic loading tests were conducted to compare HFRCC to RC columns. The results of the tests such as shear-drift angle relationship, the state of ultimate failure, and damage level at each drift angle were shown and compared. The main findings concluded from this study are as follows.

1. Use of HFRCC in columns which are expected to fail in shear improved both shear capacity and ductility, and mode of failure changes to bending failure in this tested case.
2. HFRCC is effective in shear and diagonal tension even in the ultimate design.
3. Multiple-cracks in HFRCC specimens improve the damage level.
4. Maximum story shear of HFRCC is lower than that of RC in the bending failure mode.
5. Further investigation of bending effect, ductility evaluation, and damage control is essential to develop HFRCC columns.

REFERENCES

- AIJ (1990). Design Guidelines for Earthquake Resistant Reinforced Concrete Buildings Based on Ultimate Strength Concept, Architectural Institute of Japan, (in Japanese)
- JBDPA (2001). Standard for Damage Level Classification of Reinforced Concrete Building, The Japan Building Disaster Prevention Association, (in Japanese)
- JCI (2002). Committee report on Performance Evaluation and Structural Application of Ductile Fiber Reinforced Cement Composites, Japan Concrete Institute, (in Japanese)
- AIJ (2004). Guidelines for Performance Evaluation of Earthquake Resistant Reinforced Concrete Buildings (Draft), Architectural Institute of Japan, (in Japanese)
- Nagai, S., Kaneko, T., Kanda, T., Maruta, M., (2004). Structural Performance of Damper using High Performance Fiber Reinforced Cementitious Composites. *Journal of JCI* **26:2**, 1513-1518, (in Japanese)
- Fukuyama, H. (2006). Application of High Performance Fiber Reinforced Cementitious Composites for Damage Mitigation of Building Structures. *Journal of Advanced Concrete Technology* **4:1**, 35-44